

# Influence of elevated temperature on glued-in steel rods for timber elements

Valentina Di Maria<sup>\*\*</sup>, Luca D'Andria<sup>\*</sup>, Giovanni Muciaccia<sup>\*I</sup>,  
Anton Ianakiev<sup>\*\*</sup>

*\*\* Politecnico di Milano, P.zza Leonardo da Vinci 32, Milano, Italy*

*\*\* Nottingham Trent University, Nottingham, Burton Street, UK*

*\*I Corresponding Author, E-mail: giovanni.muciaccia@polimi.it*

---

## Abstract

The load bearing capacity of Glued-in Rods (GiR) is significantly influenced by the temperature of the adhesive. This paper presents an experimental program for GiR inserted to both laminated and solid timber elements, when were subjected to elevated temperatures. Twenty-four wood specimens with a single 8mm rod glued parallel to the grain were tested to evaluate the effect of elevated temperatures on GiR performance. After applying a constant load to the bar in a pull-compression configuration, tests were conducted by increasing the ambient temperature in an electrical oven up to an appropriate level in order to avoid post-curing effects in the adhesive. Two types of resin were tested, as well as two different shapes for the internal hole surface (cylindrical and threaded), in order to evaluate whether different geometrical properties of the hole could affect the performances of the connection, when subjected to elevated temperatures. Experimental results show, that an increase in the temperature of the bonding layer causes a significant decrease in the bond shear strength of the adhesive with respect to the cold state (approximately halves when approaching the Heat Deflection). Furthermore the strength of the adhesive at elevated temperature demonstrates a clear dependence on the adhesive type and a negligible dependence on the geometry of the hole.

*Keywords:* Glued-in rods, Timber connections, Glulam timber, Adhesive anchors, Epoxy resin, Elevated temperature

---

## 1. Introduction

Glued-in rod technology is becoming increasingly popular in the construction of new timber structures and repairing of some pre-existing timber

structures. Glued-in rod timber joints provide many improvements over traditional timber joints, including lower weight, greater strength and stiffness, improved aesthetic appearance and good protection of the steel rods against corrosion and fire. The simplest method for manufacturing glued-in rod timber joints is to inject the resin into the pre-drilled hole and then insert and rotate the rod into the resin-filled hole until the rod reaches the base of the hole thus ensures a reliable bond between the rod and the timber.

Over the past four decades, a large number of experimental and theoretical studies on glued-in rod timber joints have been carried out. Most of them were pull-out tests, aimed to investigate the effects of geometrical and material properties on the pull-out strength and bond behaviour of glued-in rod joints [1].

Other research investigations analysed the effect that high temperatures have on the connection. While a few experiments were carried out to discover how a variation in the air temperature in hot climate environments could affect the mechanical performance of the adhesive connection in service, most of the research studies examined the performance of the connection under fire conditions.

Some authors in their studies [3] and [4] revealed that the adhesive lines inside timber structural members followed the outer temperature regime both, in heating and cooling phases. This phenomenon was confirmed by a Finite Element Analysis performed by [5] showing a 4/5 hours delay for the adhesive in reaching ambient temperature (Figure 1). Temperature inside roofs could reach peaks of 75 °C. The European standard [6] accepts 50 °C to be the limit between normal conditions and hot service conditions, to which different requirements were imposed concerning the adhesives performances. Currently, the European structural timber code [7] does not cover the design of structures subjected to prolonged exposure to temperatures over 60 °C. Besides, other studies ([8] and [9]) have shown that the load bearing capacity of glued-in rods significantly decreased when the epoxy resins reached an intrinsic critical temperature also called the glass transition temperature ( $T_g$ ). Once this temperature was attained, irreversible modifications of the inner structure of the polymer occurred. At this temperature, it is known that mechanical properties of the adhesive, and consequently the strength of the GiR connection, significantly decrease. Design rule proposals, predicting the pull-out strength of glued-in rods, are available [10], [1] and [11] but the effect of temperature is not taken into account in design rules.

The lack of information regarding the performance of these connections under temperature changes is still an obstacle for their use.

In past studies two different methods were frequently used to test glued-in rods (GiR) in timber at elevated temperatures. The first method is generally referred as "residual capacity test" and it involves the use of an oven to heat the connection up to a selected temperature. The connection is usually left in an oven overnight to allow the sample reach a homogeneous temperature in all its parts. Subsequently, the sample is removed from the oven and a tensile test is performed to assess its pull-out capacity.

Another method used to study GiR at elevated temperatures involves the use of a gas oven (furnace) where the sample is heated up, usually following the standard time-temperature curve of ISO 834 [12], while subjected to a constant tensile load. In Harris's [14], for example, the constant load corresponded to 30% of the design load in cold state (room temperature). These testing methods provide knowledge of the fire performance of the joint but their comparison reveals several inconsistencies. The electrical oven tests resulted in being less severe than the experiments carried out in furnace, showing failure temperatures much higher than the temperatures obtained by the furnace heating process. This inconsistency between the two aforementioned methods is mainly due to the fact that in the electrical oven the joint and therefore the adhesive are heated without being subjected to tension loads, so there is a post-curing effect; on the contrary, in the gas oven the whole adhesive connection is tested in tension under load.

However, the scope of this paper is not to assess the structural performance of a specific GiR connection, but rather to investigate the decay in the bond properties as a function of the temperature of the connection.

Such an approach is similar to the one used by Mucaccia et al [15] for post-installed rebar connections in concrete. In future, it shall be coupled with a proper design method for a GiR under temperature, which may account for a non-uniform temperature distribution along the bar, that may occur in a real design case (e.g. in a GiR used as timber reinforcement). In such cases the layer closer to the exposed surface would be expected to reach a higher temperature with respect to inner layer. Consequently, a gradient in temperature and a gradient in the bond properties as well will be expected.

In the present investigation, the samples were heated as uniformly as possible after applying a constant load. It can be assumed that, in absence of significant thermal gradients along the bar length, the decay

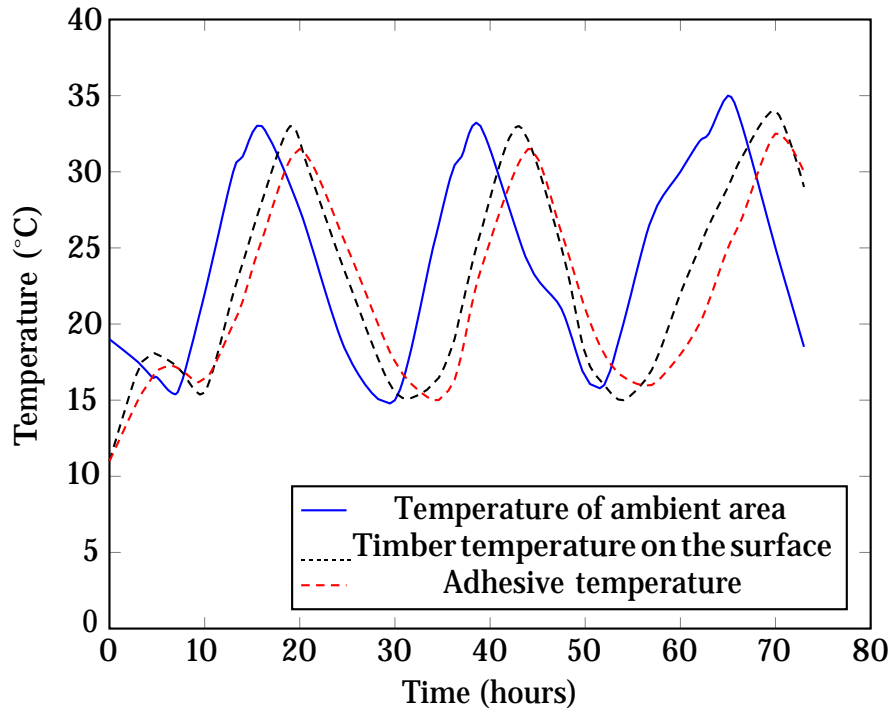


Figure 1: Relation ambient/adhesive temperature through a finite element analysis [5].

in the bond properties is uniform. Additionally, applying the load prior to temperature increases prevents the effects of post-curing, as typical in residual capacity tests.

Heating the samples after applying the load is considered a more severe method to determine the critical temperature, as many researches proved in past studies.

Preliminary tests were carried out in standard conditions ( $T = 20\text{ }^{\circ}\text{C}$  and  $HR = 65\%$ ), in order to evaluate the bond strength of the connection at cold state. Two-component epoxy resins were used to glue 8 mm steel rods into pre-drilled holes (characterised by cylindrical or threaded internal surfaces), in timber samples in order to assess the bond shear strength (hereinafter referred to simply as "bond strength") at critical temperatures. The samples were loaded applying a constant load and heated up in an electric furnace until failure.

Table 1: Material properties of timber specimens.

Type	Solid (Douglas fir)	Glulam (Spruce)
Density (kg/m <sup>3</sup> )	560	430
MC(%)	10.1	9.2

## 2. Materials and methods

### 2.1. Materials

#### 2.1.1. Timber

Two types of timber were used in the tests: solid timber (Douglas fir C16 class, according to EN338 [16]) and glulam (Spruce GL24 class, according to EN1194 [17]), whose properties are reported in Table 1. The glulam elements were obtained by cutting bigger timber blocks to the desired height. Samples of both timber species were conditioned using a climate chamber according to EN 408-2010 ([13]) for 1 week. Subsequently, before testing the specimens were weighted and moisture content was assessed by using a pin- moisture meter in order to verify equilibrium amongst all specimens.

#### 2.1.2. Steel

Threaded steel bars of grade 12.9 and diameter  $d = 8$  mm were used in this study.

#### 2.1.3. Adhesive

The adhesives used in this study were two-component epoxy resins with different viscosity values produced by the manufacturer (2K Polymer Systems Ltd). Material properties of the adhesive, provided by manufacturer, are listed in Table 2, where the HDT is the Heat Deflection Temperature.

### 2.2. Specimens and fabrication

#### 2.2.1. Geometry

The rods were inserted into the centres of the blocks of wood and glulam as shown in Figure 2. The rods were inserted at a distance from the edges to avoid splitting failure. The selected anchorage length is equal to 80 mm (i.e.  $10d$ ), while the drill-hole diameter ( $d_h$ ) is equal to 12 mm, in order to have two millimeters of glue line thickness all around the steel bar.

Table 2: Physical and mechanical properties of the epoxy resins provided by manufacturer.

	EX 1:1	EX 3:1
Density (g/cm <sup>3</sup> )	1.7	1.5
Compressive strength (24 hours) (MPa)	75	75
Tensile strength (24 hours) (MPa)	18	18
Flexural strength (24 hours) (MPa)	45	45
HDT (7 days) (°C)	49	49
Viscosity (20 °C) (Pa s (daP)) ±50	240	720

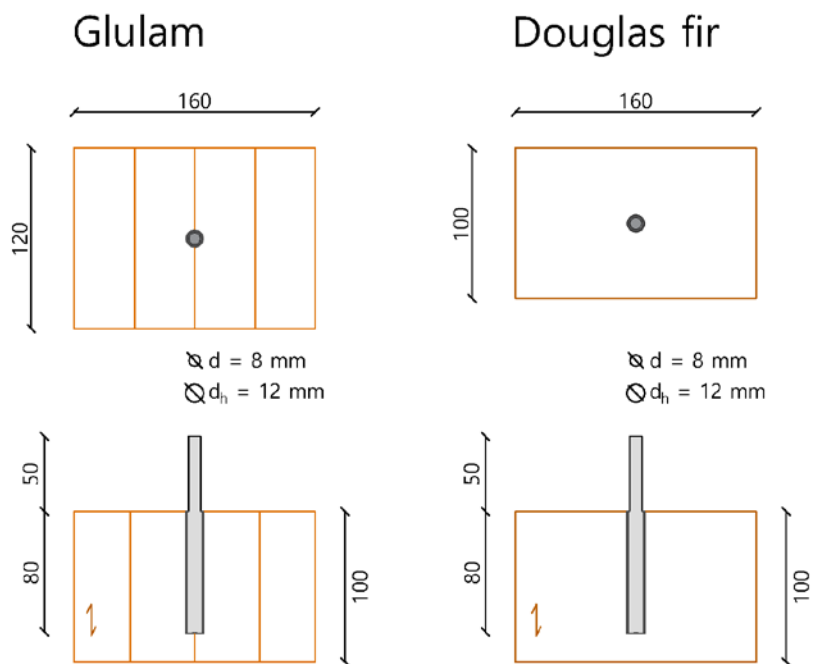


Figure 2: Glulam and Douglas fir samples.



Figure 3: Installation procedure.



Figure 4: Cylindrical vs. Threaded hole

### 2.2.2. Fabrication of specimens

Holes were manually drilled parallel to the wood grain.

Both threaded internal and traditional cylindrical hole shapes were manufactured to evaluate whether a GiR with different geometrical properties of the bore hole would perform differently at both cold and elevated temperatures. Both specimen types were manufactured by following the installation method listed below:

- drill a first hole choosing the steel bar diameter and a depth length that is 1 cm deeper than the desired final embedment length;
- drill a second hole to the designed shape, diameter and depth;
- clean the hole;
- inject the adhesive;
- insert the threaded steel bar twisting with a back and forth movement until the bar reaches the end of the hole;
- insert a specific plastic support ring through the steel bar to the joints surface. This support will help the bar to maintain a vertical position during the resin curing phase.

The cylindrical shape holes were made by a traditional drill bit for woodworking whereas the threaded shape was made by drilling a screw in and out of the wooden surface.

Grease was not present in the borehole; however, prior to injection, holes were cleared from any timber dust by several blows and brushes before gluing the steel bar. Epoxy resin adhesives were injected into the pre-drilled holes from the bottom to the top using an application gun, following the installation method suggested by the manufacturer [18] and [19] (Fig. 3). The bottom part of the borehole, as it is shown in Figure 4, is characterised by a reduced hole diameter in order to provide a base for the steel bar insertion. Furthermore the insertion of a plastic support ring through the steel bar to the joint's surface allowed the bar to maintain a perfect vertical position during the resin curing time. The aforementioned technical solutions, adopted during the joint's manufacturing phase, led to having a uniform glueline thickness of the adhesive along the entire embedded length of the steel bar.

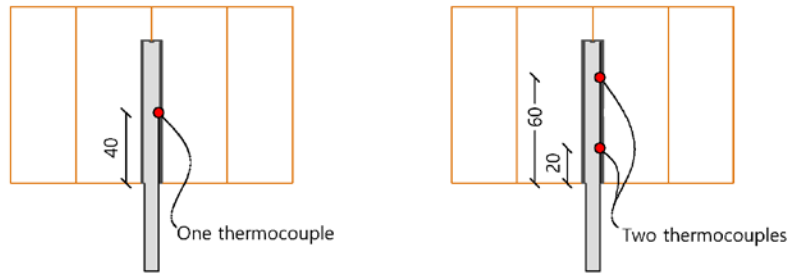


Figure 5: Thermocouples position.

The threaded steel bars were then inserted twisting with a back and forth movement to ensure no voids in the resin along the glue line. Finally, during the curing process the specimens were kept in a room at temperature  $T = 20 \pm 2^\circ\text{C}$  and relative humidity  $RH = 65 \pm 5\%$  for the entire curing time. The curing time provided in the adhesive datasheet was increased up to 36 hours to achieve full cure.

The adopted installation method is suitable for relatively short bonded length, as in the described experiments. For longer bonded lengths, more advanced techniques may be used to assure a proper filling with no voids along the glue line, Steiger et al. [2].

The temperature inside the resin member was measured through the use of thermocouples. For samples characterized by the threaded hole shape only one thermocouple was inserted, due to the small interspace between the rod and the hole surface. Two thermocouples at different heights were inserted in samples characterized by the cylindrical hole shape such to monitor the distribution of the internal temperature along the rod (Fig. 5).

### 2.2.3. Pull-out tests at cold state

Initially, pull-out tests were performed at normal ambient temperature to evaluate the resistance of the connection in standard environmental conditions. All the tests were displacement controlled. The displacement rate was  $0.03\text{mm/s}$ . Test results are reported in Table 3, where all the samples are listed with a denotation: AA BB C DDD E. It refers to:

- AA represent the type of timber → GL for Glulam timber, FIR for Douglas fir
- BB represent the embedment depth → 80mm

- C represent the shape of the hole → C for Cylindrical, T for Threaded
- DDD represent the Epoxy type → EX1 for Epoxy 1, EX3 for Epoxy 3
- E represent the number of the sample → 1,2,3

In the same Table:

- $N_u$  is the maximum pull-out force
- $\tau_u$  is the maximum shear stress, evaluated according to Equation 1
- $\tau_{u,m}$  is the mean value of the maximum shear stress of the series
- $\delta_u$  is the ultimate slip (peak point)
- $\delta_{u,m}$  is the mean value of the ultimate slip of the series

Sample FIR 80 T EX3 3 has been tested but unfortunately, data was not recorded by the system.

Figure 6 reports representative tangential stress - slip curves for the two types of epoxy resins. The connection capacity was reached soon after over-coming the proportionality limit by bond failure. For all the samples failure occurred at the adhesive-timber interface.

After the peak, a quite steep descending branch was detected while the bar is progressively pulled out of the timber substrate. The system showed a very limited capacity of redistributing loads, thus resulting in a globally brittle behavior. In all the tests high values of the maximum tangential stress in the range 11 to 13 MPa were reached. The presence of an unloading cycle at a deformation of approximately 2.5 mm is a common aspect of all the performed tests and it is due to a loss of load for very high displacement, probably induced by micro cracking in the base material. Stresses are calculated assuming a constant shear stress acting on the lateral surface of the bar, according to the following uniform bond model:

$$\tau_u = \frac{N_u}{\pi \cdot d \cdot h_{eff}} \quad (1)$$

where:

- $\tau_u$  is the maximum shear stress
- $N_u$  is the maximum pull-out force

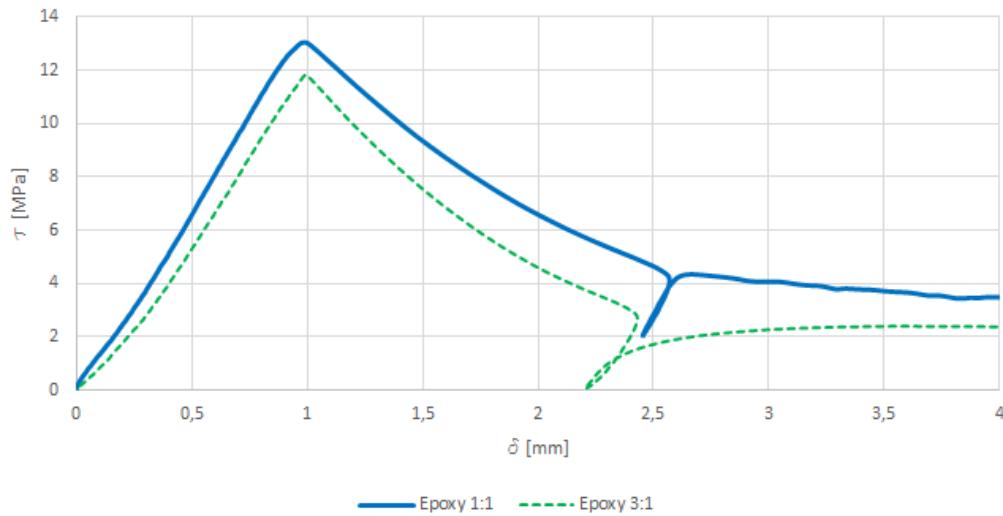


Figure 6: Representative stress-slip curves for Epoxy 1:1 and Epoxy 3:1.

- $d$  is the rod diameter
- $h_{eff}$  is the embedment length

No significant differences were detected in the pull-out behavior between cylindrical and threaded hole samples except for the anchors made from Douglas Fir and glued by low viscosity epoxy (EX 1:1) which presented a slight increase in the pull-out loading capacity.

The obtained results are quite different with respect to similar findings available in the literature [5], [10], [1], which implicitly account also for the effect of bar spacing or edge distance. On the contrary, in the proposed approach tests are carried out on single rods installed in a timber specimen wide enough to prevent splitting along the bar, thus determining the connections properties independently on the effect of close edges or of closely spaced rods.

#### 2.2.4. Equipment and experimental procedure

A constant load was applied to the samples during the heating process in the electric furnace that was 50% of the average failure loads, obtained by pull-out tests in cold state, representing an approximate design load for the connection.

The 50% level was chosen as an approximate ratio between the nominal (characteristic) value of action  $S_k$  and the mean value of resistance

Table 3: Pull-out test results at cold state.

Sample	$N_u$ [kN]	$\tau_u$ [MPa]	$\tau_{u,m}$ [MPa]	$\delta_u$ [mm]	$\delta_{u,m}$ [mm]
GL_80_C_EX1_1	26.3	13.1		0.98	
GL_80_C_EX1_2	28.1	14.0	13.0	1.18	1.05
GL_80_C_EX1_3	23.8	11.8		0.99	
GL_80_T_EX1_1	23.5	11.7		1.03	
GL_80_T_EX1_2	26.5	13.2	12.8	1.09	1.08
GL_80_T_EX1_3	27.4	13.6		1.10	
GL_80_C_EX3_1	23.5	11.7		1.07	
GL_80_C_EX3_2	20.8	10.4	12.6	0.78	1.00
GL_80_C_EX3_3	31.4	15.6		1.15	
GL_80_T_EX3_1	23.8	11.8		1.00	
GL_80_T_EX3_2	19.3	9.6	11.2	0.76	0.93
GL_80_T_EX3_3	24.2	12.0		1.02	
FIR_80_C_EX1_1	25.3	12.6		4.58	
FIR_80_C_EX1_2	28.0	13.9	13.3	5.33	4.55
FIR_80_C_EX1_3	27.1	13.5		3.73	
FIR_80_T_EX1_1	29.4	14.6		5.20	
FIR_80_T_EX1_2	29.7	14.8	14.7	5.39	5.23
FIR_80_T_EX1_3	29.7	14.8		5.11	
FIR_80_C_EX3_1	27.2	13.5		3.82	
FIR_80_C_EX3_2	27.8	13.8	13.2	4.45	3.98
FIR_80_C_EX3_3	24.7	12.3		3.68	
FIR_80_T_EX3_1	23.7	11.8		3.37	
FIR_80_T_EX3_2	20.1	10.0	10.9	2.79	3.08
FIR_80_T_EX3_3	/	/		/	

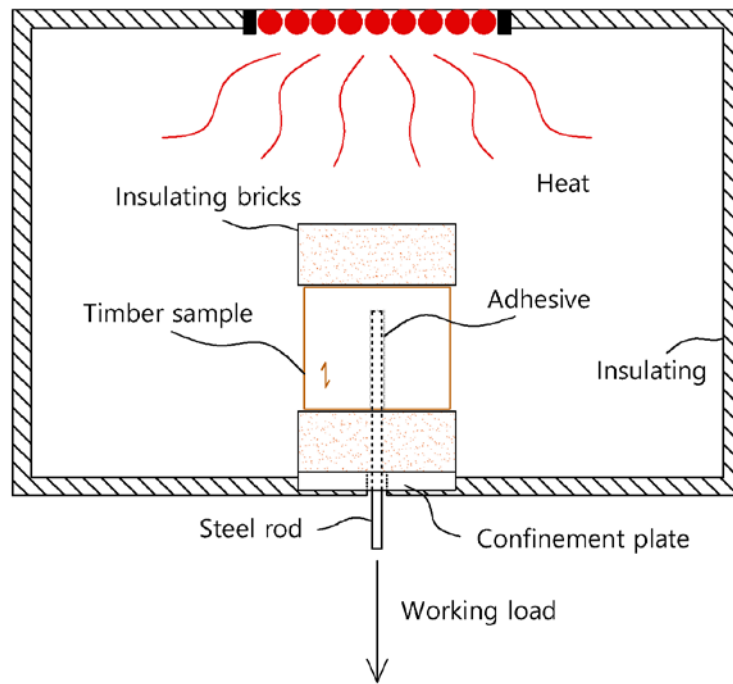


Figure 7: Oven scheme.



Figure 8: Oven details.

$R_m$  according to the relationship  $\gamma_f \times S_k = R_m \times (1 - 1.645 \times v) / (\gamma_m)$  (where  $v$  is the Coefficient of Variation of test results at cold state, assumed as representative of the connection behavior, and  $\gamma_f$  and  $\gamma_m$  are partial safety factors for action and resistance, taken as equal to 1.4 and 1.35, respectively).

Three samples for each joint type were assembled and tested, samples properties are reported in Table 4. The installation of some samples in the electric furnace was unsuccessful due to some imperfections of the insulating brick located between the sample and the confinement steel plate. Specifically, no perfect vertical alignment of the specimen was achieved and for this reason the sample, during the loading phase, prematurely failed. Such results are not reported.

The tests were conducted using an electric furnace where samples of adhesive connections were tested in pull-compression test regime under a constant load (Fig. 7 and 8). The pull-out capacity of the samples was tested in pull-compression (confined) conditions using a confinement steel plate with a hole diameter of 18 mm. The samples were covered with some insulating bricks, in order to have an homogeneous distribution of the temperature inside the base material.

A closed-loop servo hydraulic testing machine with 100 kN load capability under displacement control was used. Load was acquired with a 50 kN class I load cell while the slip at the loaded end was monitored by two 100mm LVDTs (repeatability error 0.67%) placed symmetrically at the two sides of the rod. All data were acquired with a HBM Spider8 data acquisition system. Temperature in the electric furnace was raised up to 150 °C in 30 minutes and left constant until specimen failure occurred (Fig. 9). Some samples had been heated by using a different time-temperature curve which is identified by a linear heating trend. In this specific case, an increase of 100 °C in temperature was set every 20 minutes (Fig. 10). It is important to underline that the test set up was chosen in order to prevent the steel bar from being heated directly during the test. Therefore, the heating process of the connection took place only by transmission of heat from the outside toward the inside through the timber or glulam.

### **3. Results and discussion**

Tests results are reported in Table 5. It is initially noticed how temperatures at failure are dependent on the epoxy resin used in the connections. The bond strength of samples made of EX 3:1 showed slightly

Table 4: Samples features and selected constant load values for tests at elevated temperatures.

Sample	Epoxy type	Hole type	Timber type	Load [kN]
DF_80_C_EX1_1	EX 1:1	Cylindrical	Douglas fir	13.6
DF_80_C_EX1_2	EX 1:1	Cylindrical	Douglas fir	13.3
DF_80_C_EX1_3	EX 1:1	Cylindrical	Douglas fir	13.6
DF_80_T_EX1_2	EX 1:1	Threaded	Douglas fir	14.6
DF_80_T_EX1_3	EX 1:1	Threaded	Douglas fir	14.5
GL_80_C_EX1_1	EX 1:1	Cylindrical	Glulam	12.9
GL_80_C_EX1_2	EX 1:1	Cylindrical	Glulam	13.0
GL_80_C_EX1_3	EX 1:1	Cylindrical	Glulam	13.0
GL_80_T_EX1_2	EX 1:1	Threaded	Glulam	13.1
GL_80_T_EX1_3	EX 1:1	Threaded	Glulam	13.1
DF_80_C_EX3_1	EX 3:1	Cylindrical	Douglas fir	13.0
DF_80_C_EX3_2	EX 3:1	Cylindrical	Douglas fir	13.0
DF_80_C_EX3_3	EX 3:1	Cylindrical	Douglas fir	13.0
DF_80_T_EX3_1	EX 3:1	Threaded	Douglas fir	11.0
DF_80_T_EX3_2	EX 3:1	Threaded	Douglas fir	11.0
DF_80_T_EX3_3	EX 3:1	Threaded	Douglas fir	11.0
GL_80_C_EX3_1	EX 3:1	Cylindrical	Glulam	10.0
GL_80_C_EX3_3	EX 3:1	Cylindrical	Glulam	10.1
GL_80_T_EX3_1	EX 3:1	Threaded	Glulam	11.0
GL_80_T_EX3_2	EX 3:1	Threaded	Glulam	11.0
GL_80_T_EX3_3	EX 3:1	Threaded	Glulam	11.0
- - - -				
- - - -				
- - - -				
- - - -				

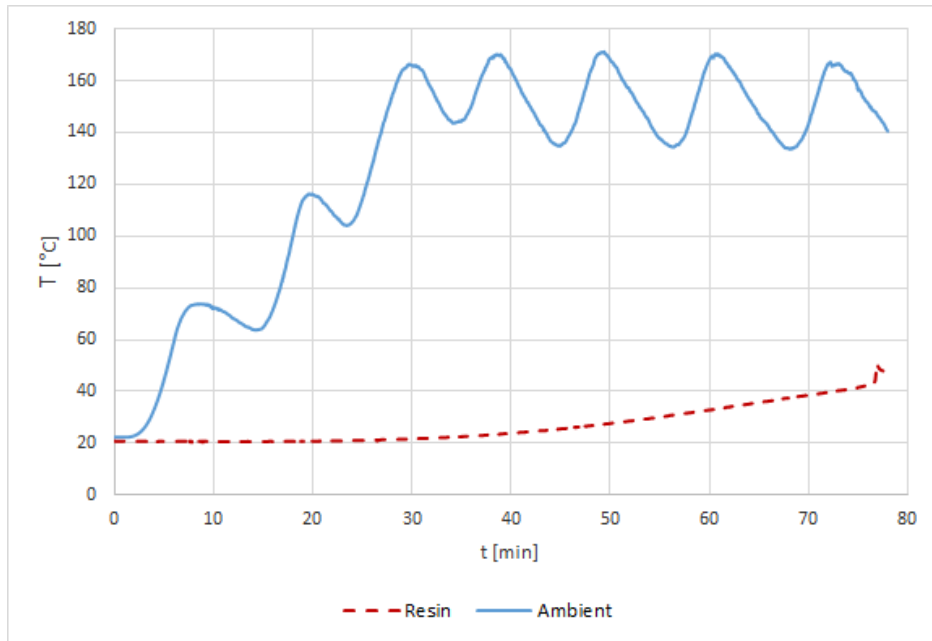


Figure 9: Resin and Ambient (oven) temperature's trend 1.

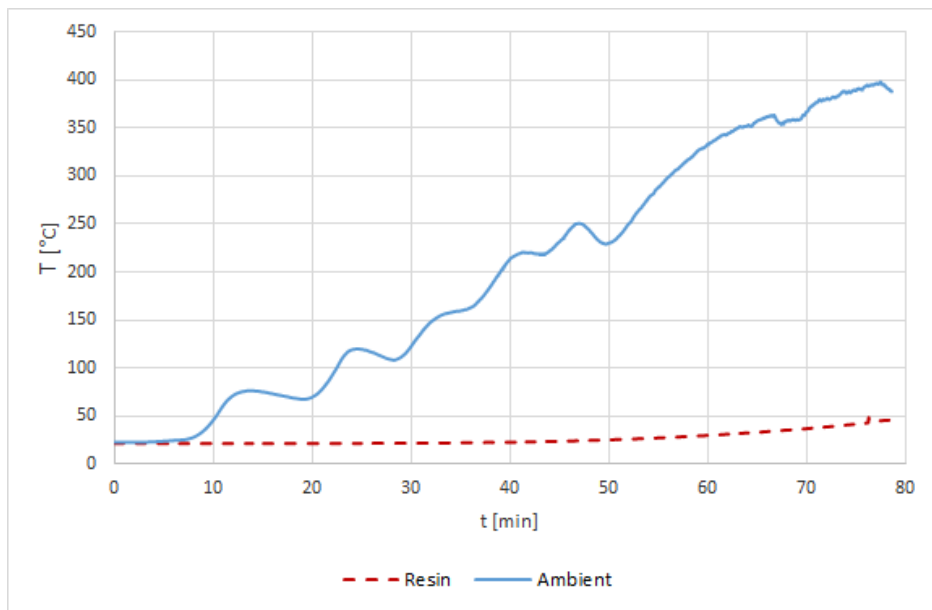


Figure 10: Resin and Ambient (oven) temperature's trend 2.

Table 5: Test results at elevated temperatures.

Sample	$\tau_u$ [MPa]	$\tau_{u,m}$ [MPa]	$T$ [°C]	$T_{av}$ [°C]	$\delta_u$ [mm]
DF 80 C EX1 1	6.77		45.6		2.83
DF-80-C-EX1-2	6.61	6.71	43.6	46.4	2.81
DF-80-C-EX1-3	6.76		49.9		3.42
- - - -					
DF 80 T EX1 2	7.27		48.6		2.33
DF 80 T EX1 3	7.21	7.24	48.7	48.7	2.55
GL-80-C-EX1-1	6.43		39.2		0.61
GL-80-C-EX1-2	6.47	6.46	42.9	42.8	2.10
GL-80-C-EX1-3	6.47		46.4		2.71
- - - -					
<b>GL 80 T EX1 3</b>	<b>6.42</b>	6.51	<del>43.2</del> 43.8	43.5	<del>1.41</del> 2.06
DF 80 C EX3 1	6.47		51.8		2.90
DF-80-C-EX3-2	6.47	6.47	50.8	54.2	3.19
DF-80-C-EX3-3	6.47		59.9		3.66
DF-80-T-EX3-1	5.47		56.1		2.17
DF-80-T-EX3-2	5.47	5.47	59.2	57.8	2.83
DF-80-T-EX3-3	5.47		58.0		2.28
- - - -					
- - - -					
GL 80 C EX3 1	4.98		45.4		2.85
GL 80 C EX3 3	5.00	4.99	54.1	49.7	3.27
GL-80-T-EX3-1	5.47		50.6		2.40
GL_80_T_EX3_2	5.48	5.48	39.6	50.6	1.52
GL_80_T_EX3_3	5.49		54.1		2.40
- - - -					

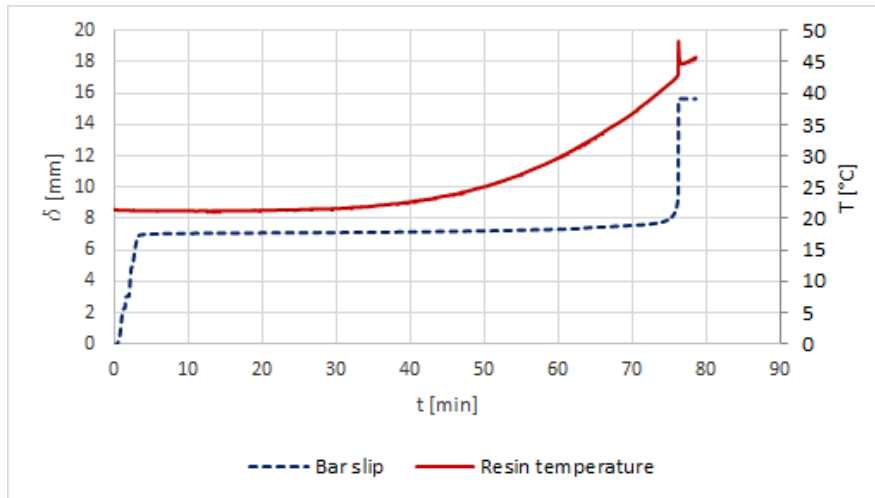


Figure 11: Evolution of temperature with time for air oven temperature (ambient) and at adhesive location(resin)

lower values than the EX 1:1 specimens due to the lower constant load applied during the tensile test. The high viscosity of EX 3:1 at cold state affected the bonding quality providing adhesive connections with lower capacity than samples made of EX1:1.

The detected variation of the temperatures at failure for the same load level are consistent with previous results of bonded anchors in concrete when approaching the glass transition temperature of the adhesive Mucaccia et al [15].

At elevated temperatures, the failure temperature reached by the samples made of EX 1:1 and EX 3:1 were not affected by the shape of the internal borehole as it is mainly influenced by the thermal properties of the adhesives. Therefore, no significant differences were identified between the performance of cylindrical and threaded samples at elevated temperatures. Although cylindrical and threaded samples were characterised by a different internal shape, they both had a maximum internal diameter of equal size (12mm). Hence, in both types the adhesive layer was "protected" by the same amount of wood when subjected to elevated temperatures.

The increase in the temperature at rod location is shown in Figure 11. It also shows how the slip of the rod initially increases due to load application and it is almost constant until a given temperature is reached. For the selected load level, the temperature is close to the Heat Deflection Temperature provided by the manufacturer (see Table 2).



Figure 12: “crumbling effect” in the epoxy resin after being exposed to elevated temperatures.

In the case of the heated samples, it was not possible to place the displacement transducers near to the timber surface. Consequently, the displacement reported in Table 5 also includes the elastic extension of the portion of the bar located outside the oven. Such effect varies as a function of the applied load and, consequently, of the bond stress and it is equal to  $0.0723\text{mm/MPa}$  resulting in a maximum value of  $0.52\text{mm}$  for the most loaded sample.

A visual analysis of the samples after testing showed how all the samples present a predominant failure mode which can be classified as a bond failure at the steel-adhesive interface.

Observation of the samples after failure show a visible change in the epoxy texture, a “crumbling effect” of the adhesive in the connection, due to a critical increase in temperature combined with the application of a tension load. Such observation proves that the samples failures occurred in the connection due to a loss in strength of the thermosetting materials (Fig. 12). Similar results were also observed by Harris [14].

Figure 13 finally shows the decay in the bond strength for both adhesives and hole shapes. Two load levels were investigated and the results indicated that the bond strength halves when the HDT of the adhesive is approached, with slightly higher temperatures for the solid Douglas FIR timber with respect to the Spruce Gluelam. A clear dependence of the performance of the GiR at elevated temperature on the adhesive type can then be inferred.

The proposed approach can be generalized, extending the investigation to a different value of applied load and to derive a complete bond strength vs temperature curve for a specific adhesive and eventually, timber type.

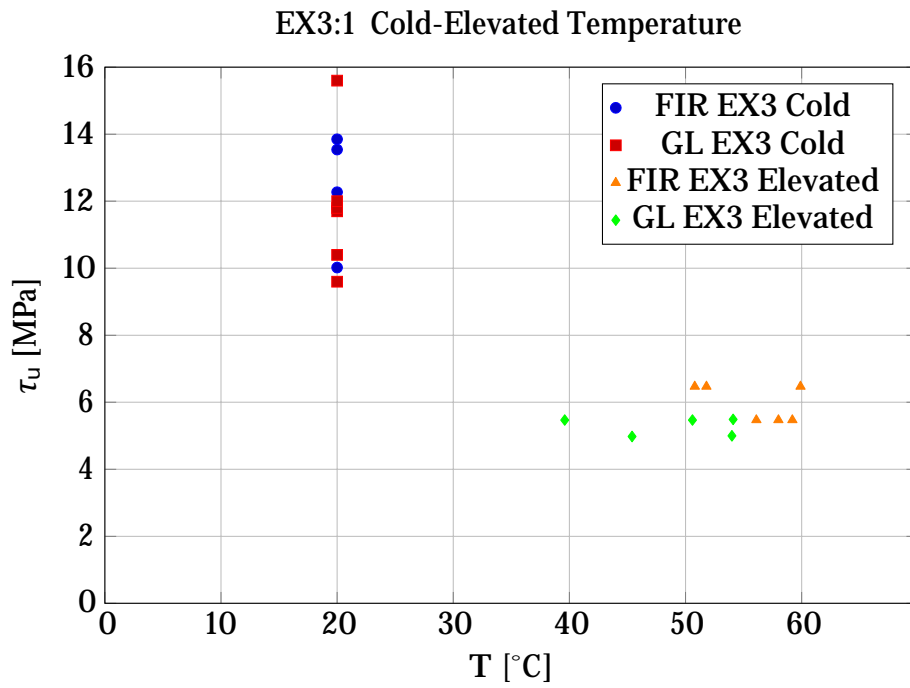
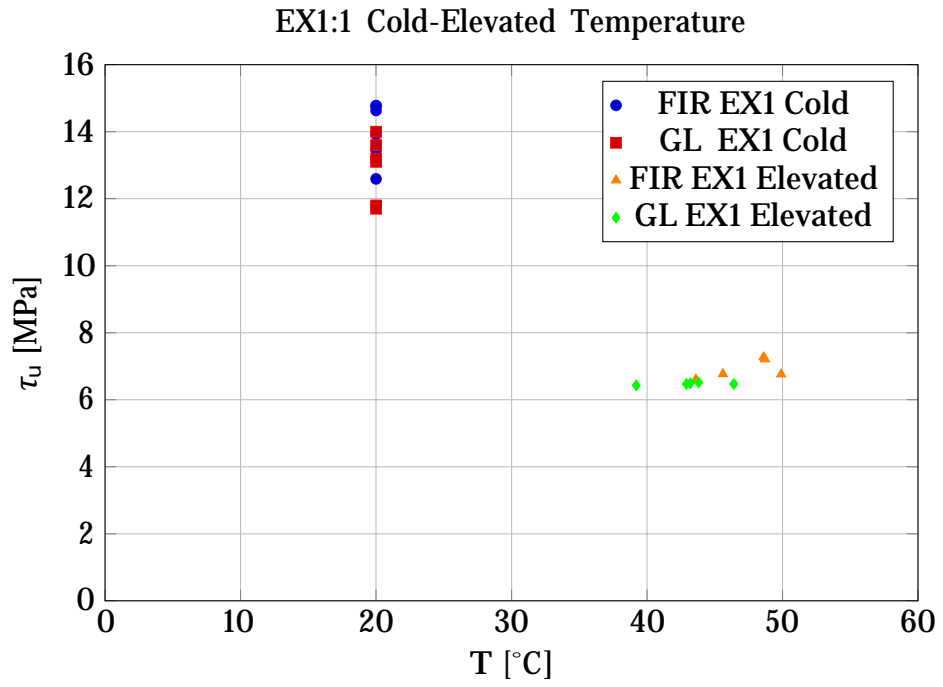


Figure 13: Bond strength depending on temperature.

#### 4. Conclusions

When designing Glued in Rods (GiR) it is essential to consider how an increase in temperature due to both a fire event or a solar heating process might affect its structural performance in situ.

The scope of the paper does not assess the structural performance of a specific GiR connection, but rather investigates the decay in the bond properties as a function of the temperature which may be reached at a location of the GiR. In the presented investigation, two different types of epoxy resins were used as adhesive for 8mm steel rods glued to laminated or solid timber subjected to elevated temperature. Load was kept constant during the temperature increase at a level approximately equal to service load.

It was found that the selected electric furnace allowed a uniform distribution of temperature along the bar and it represents a valid apparatus to detect the decay in bond properties of the connection. The application of a constant load prior to the temperature increase avoids post-curing effects of the adhesives. However, negative effects of creep may be induced.

It is shown that an increase in the temperature at the bonding layer causes a significant decrease in the bond strength of the adhesive with respect to the cold state, thus the performance of the connection at elevated temperatures is highly dependent on the thermal properties of the adhesive used to assemble it.

No significant difference was found for cylindrical or threaded shape drilled holes. When varying the timber type, a trend is noticeable on failure temperatures for both adhesives, showing the Douglas FIR had generally higher failure temperatures than the Spruce Glulam.

It can be expected that for different values of the applied load, different values of temperature at failure may be detected. Investigating such variables further may allow in the future to derive a complete bond strength vs temperature curve for a specific GiR typology. However, a specific design method which may account for a temperature gradient along the bar in a real design case and, consequently, for a non-uniform distribution of the bond strength along the bar still has to be developed.

#### References

- [1] R Steiger, E Gehri, and R Widmann. Pull-out strength of axially loaded steel rods bonded in glulam parallel to the grain. *Materials and structures*, 2007.

- [2] Steiger R., Serrano E., Stepinac M., Rajcic V., O'Neill C., McPolin D., and Widmann R. Strengthening of timber structures with glued-in rods. *Construction and Building Materials* 97 90105, 2015
- [3] S Aicher, D Kalka, and R Scherer. Transient temperature evolution in glulam with hidden and non-hidden glued-in steel rods. *Otto-Graf-Journal*, 2002.
- [4] H Cruz and J Custodio. Thermal performance of epoxy adhesive in timber structural repair. *Proceedings of the 9th world conference on timber engineering. Portland, USA, 2006.*
- [5] C Faye and L LeMagorou. French data concerning glued-in rods. *In proceedings of the CIB-W18 Meeting Thirty-Seven 37-7-10. Edinburgh, Scotland, 2004.*
- [6] EN301. European Committee for Standardization (CEN). Adhesives, phenolic and aminoplastic for load-bearing timber structures: classification and performance requirements. 2013.
- [7] EC5. European Committee for Standardization (CEN). Eurocode 5: design of timber structures, EN 1995. 2004.
- [8] SAicher and G Dill-Langer. Influence of moisture, temperature and load duration on the performance of glued-in rods. *Proceedings of the international RILEM symposium on joints in timber structures. Stuttgart, Germany, 2001.*
- [9] J Custodio, JG Broughton, and H Cruz. A review of factors influencing the durability of structural bonded timber joints. *International Journal of Adhesion and Adhesives*, 2009.
- [10] HRiberholt. Glued bolts in glulam-proposals for CIB code. *Proceedings of the 21st conference of CIB-W18. Parksville, Canada, 1988.*
- [11] R Widmann, R Steiger, and E Gehri. Pull-out strength of axially loaded steel rods bonded in glulam perpendicular to the grain. *Materials and structures*, 2007.

- [12] ISO834. International Standards. Fire resistance tests - Elements of building construction. 2014.
- [13] UNI408. European Committee for Standardization (CEN). Timber structures. Structural timber and glued laminated timber. Determination of some physical and mechanical properties 2012.
- [14] S Harris. Fire resistance of epoxy-grouted steel rod connections in laminated veneer lumber (lvl). *Fire Engineering Research Report 04/07*, 2004.
- [15] G Muciaccia, A Consiglio, and G Rosati. Behavior and design of post-installed rebar connections under temperature. *Key Engineering Materials. Vol. 771, pp 783-790*, 2016.
- [16] EN338. European Committee for Standardization (CEN). Structural timber - Strength classes. 2009.
- [17] EN1194. European Committee for Standardization (CEN). Timber structures. Glued laminated timber - Strength classes and determination of characteristic values. 2000.
- [18] 2K Polymer Systems Limited. *EX1 pure epoxy - Product Data Sheet*.
- [19] 2K Polymer Systems Limited. *EX3 pure epoxy - Product Data Sheet*.